

Photobleaching and reorientational dynamics of dyes in a nematic liquid crystal

M. Nöllmann and D. Shalóm

Instituto Balseiro, Universidad Nacional de Cuyo, 8400 San Carlos de Bariloche, Río Negro, Argentina

P. Etchegoin and J. Sereni

Centro Atómico Bariloche and Instituto Balseiro, Comisión Nacional de Energía Atómica and Universidad Nacional de Cuyo, 8400 San Carlos de Bariloche, Río Negro, Argentina

(Received 25 August 1998)

The polarized fluorescence of excited dyes in a prototype nematic liquid crystal is studied as a function of temperature, polarization of the light, and laser wavelength. We show explicitly the coexistence of photobleaching and dye diffusion through the nematic host as two mechanisms influencing the magnitude of the fluorescence signal. In addition, we exhibit clear evidence of the presence of a torque at low input laser powers that twist the dye molecules with respect to the director orientation of the liquid crystal, if the dyes are resonantly excited. The fluorescence emission in this latter case is able to perceive the birefringence of the nematic liquid crystal host, and this is shown as clear oscillations in the polarized fluorescence as a function of temperature. Extensive qualitative comparisons of the experimental results with the mean-field Maier-Saupe theory of the nematic state are presented, and a model is proposed to account for the observations. [S1063-651X(99)10802-X]

PACS number(s): 61.30.Gd, 87.64.Ni, 78.20.Fm, 32.80.Lg

I. INTRODUCTION AND OVERVIEW

Dye doped liquid crystals exhibit a myriad of optical effects which are intrinsic to their unique nature. Originally, the orientation of dichroic dyes by the cooperative alignment of the liquid crystal (LC) molecules in the nematic phase was discovered by Heilmeyer, Castellano, and Zanoni [1], who designated the effect as *guest-host interaction*. By measuring the polarized fluorescence of the dyes, the method was immediately recognized as a powerful tool to gain microscopic information on the different liquid crystalline phases [2]. The guest-host effect has also been used for tailor-made electro-optical LC devices with improved contrast ratios at specific wavelengths in the visible [3,4]. More recently, enhanced light-induced molecular reorientations in dye doped LC's were observed, and their understanding in terms of a microscopic interaction between the excited dyes and the LC molecules was developed by the pioneering work of Jánossy [5]. It turns out that a light beam acting on a dye doped LC may display an optical torque which is 2–3 orders of magnitude larger than the usual one, which is proportional to the dielectric anisotropy of the LC molecules. This effect has dramatic consequences for the threshold of the optical Fréedericksz transition [5]. The enhanced nonlinear optical properties and the variety of phenomena observed in dye doped LC's have recently triggered several studies. Notwithstanding, many of the details of the observed phenomena, as well as their relationships, are not fully worked out. Moreover, as pointed out by Jánossy [6], the connection between the microscopic molecular properties of the dyes and LC's and the resulting macroscopic optical nonlinearities is not yet understood.

Among the most salient results reported in the literature of dye doped LC's we highlight the following: Khoo and co-workers [7] reported the existence of a negative reorientational effect in the transient regime of a dye doped nematic LC after a short laser pulse illumination. Fundamental as-

pects of the order parameter in the nematic and smectic-A phases using the guest-host effect were reported by Bauman and Wolarz [8] using polarized fluorescence and absorption, and by Wu [9] using second harmonic generation. The photochromism of azo dyes and their effect on liquid crystalline ordering was reported by Blinov *et al.* [10], while the fundamental aspects of the optical torque enhancement in bulk dye doped LC's were principally studied by Jánossy and co-workers [5,6,11] and Shen and co-workers [12]. From the standpoint of applications, dye doped liquid crystals were investigated as possible candidates for optical cavities [13] as well as spatial filtering [14,15], photothermal self-phase modulation [16], holograms [17,19], and optical recording [18,20]. Surface-mediated alignment in dye doped LC's under laser light illumination was reported by Gibbons *et al.* [21]. In the latter work, the alignment of the LC becomes perpendicular on a macroscopic scale to the electric field polarization of the laser, presumably by the indirect action of the dye and the aid of the surface interaction. It is worth noting at this stage that several of the dye-assisted reorientational mechanisms delineated in the literature are not necessarily equivalent or related to each other. The transient reorientation observed in Ref. [7] is, in the simplest possible approach, not related to the enhanced optical torque seen under constant wave laser illumination in Ref. [5]. Likewise, the surface-assisted reorientation used for pattern recording by optical means in Ref. [21] seems to be specifically related to the presence of a boundary. In fact, the reversible surface-mediated optical alignment in a dye doped LC reported in Ref. [21] is such that the molecules orient themselves in a direction perpendicular to both the electric field of the light \vec{E} and the director field \vec{n} in a planar aligned LC cell. Conversely, the enhanced bulk optical torque influencing the optical Fréedericksz transition in Ref. [5] is found to be proportional, and to have the same sign as the normal optical torque exerted by the laser, implying that the molecules will

tend to straighten along \vec{E} for LC's with a positive dielectric anisotropy. Finally, the transient reorientational regime in Ref. [7] indicates a torque that directs the LC molecules perpendicular to \vec{E} , but along the propagation direction of the laser \vec{k} .

These caveats aside, it is fairly well established that the different optical reorientations reported in the literature have one feature in common—to wit, the simultaneous action of the dyes coupled to the optical field of the laser and the interaction of the LC molecules with the excited dyes at a molecular level. This is the basis of the molecular interpretation of bulk absorption-induced optical reorientation processes in dye doped LC's developed by Jánossy [5].

In this paper, we present a comprehensive study of polarized fluorescence from resonantly excited dyes in a prototype nematic LC for low excitation powers. We shall show clear experimental evidence of the existence of polarized photobleaching under resonant excitation in the nematic state, as well as selective coupling of the laser light producing a rotation of the dyes *with respect to the nematic host* at low powers. Extensive comparisons with simple models based on the mean-field Maier-Saupe theory [22] of the nematic state are presented when necessary. The existence of a stable fluorescence photobleached signal is forthwith associated with the presence of dye diffusion through the nematic host. We performed an independent optical experiment to measure the diffusion coefficient of the dyes, and to gain an understanding of the photobleaching process. In addition, we show that the twisting of the dyes with respect to the nematic host is a resonance phenomenon which depends not only on the excitation wavelength but also on the power density of the laser.

The paper is organized as follows: Section II presents different subsections with the setups for the various experiments and their results. A brief description of their interpretation with the necessary theoretical background is given in each subsection. The main results and the discussion about their origins are gathered in Sec. III and, finally, in Sec. IV a few conclusions are bestowed.

II. EXPERIMENTS

A. Outline

Let us briefly commence with the following *gedanken experiment*: a small quantity of a dichroic dye is dissolved into a nematic LC well below the solubility limit, and a cell with planar alignment is prepared with the mixture. If the LC is in the nematic phase, it is expected to orient the elongated dye molecules along the director \vec{n} through the guest-host interaction and, consequently, the absorption of the LC cell becomes anisotropic. Let us consider the most frequent case of a dichroic dye which predominantly absorbs and emits for an optical field polarization parallel to its long axis, that is to say, parallel to \vec{n} . The situation is schematically depicted in Fig. 1(a), where a mixture of LC and dye molecules is shown to have an average orientation along \vec{n} , forced upon by the internal elastic energy of the LC and the boundary conditions of the planar alignment. Suppose that a laser impinges upon the sample with a polarization parallel to \vec{n} , i.e., along the direction of maximum absorption and fluorescence emission,

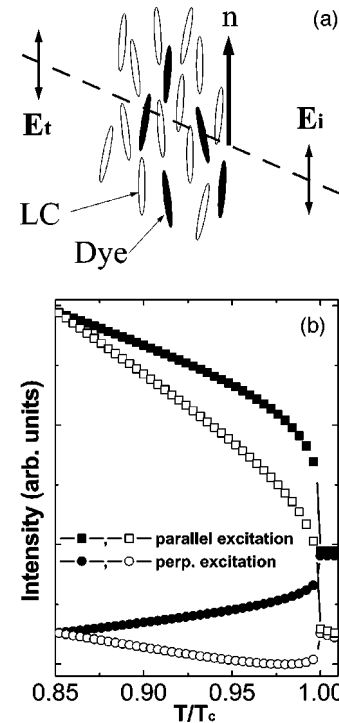


FIG. 1. (a) Schematic representation of a dye doped LC cell with planar alignment shone by an incident laser with polarization along \vec{E}_i . The average orientation of the molecules is along the director \vec{n} . The fluorescence emission of the molecules is analyzed along $\vec{E}_t \parallel \vec{n}$ by a polarizer. We shall refer to this situation as *parallel excitation*. By rotating the LC cell by 90° along the propagation direction of the laser, we achieve the *perpendicular excitation* condition. (b) Model fluorescence emission from the dyes for both excitation conditions. The average geometric factors in Eqs. (1) and (2) are evaluated by means of the Maier-Saupe model. Solid (open) symbols correspond to the model without (with) corrections for nonradiative recombinations.

its frequency being above the absorption edge of the dyes. Furthermore, let us assume that we analyze the fluorescence emission of the dichroic dyes along \vec{n} . In what follows, we shall refer to a situation like the one depicted in Fig. 1(a) as *parallel excitation*. If the liquid crystal cell is rotated by 90° along the propagation direction of the laser in Fig. 1(a), the molecules should neither absorb nor emit, except for the fact that the alignment along \vec{n} is of course not strict at a finite temperature T but rather smeared out by the thermal spread of orientations around \vec{n} . Henceforth, we shall refer to this second situation as *perpendicular excitation*.

Consider first the case of parallel excitation. Every single dye molecule with a small deviation Θ from \vec{n} will gain an excitation proportional to the absorption coefficient at the laser frequency and to the projection of \vec{E} along its long axis, i.e., $\propto I_0 \cos^2(\Theta)$ and $I_0 \propto E^2$. This latter factor takes into account the amount of excitation being produced on the molecule. On the other hand, since the light let off by the dyes is analyzed along the same direction by a polarizer, there is an additional factor $\propto \cos^2(\Theta)$ for the intensity reaching the detector. The measured intensity for parallel excitation is therefore expected to be

$$I_{\parallel}(T) \propto I_0 \langle \cos^4(\Theta) \rangle_T, \quad (1)$$

where $\langle \rangle_T$ denotes a thermal average at a temperature T . By the same reasoning, for the perpendicular excitation we obtain

$$I_{\perp}(T) \propto I_0 \langle \sin^4(\Theta) \rangle_T, \quad (2)$$

where we expect $I_{\parallel}(T) > I_{\perp}(T)$ for T below the critical transition temperature from the nematic to the isotropic state T_c .

For the purpose of modeling and a general comparison with the experiment, let us consider what the thermal averages in Eqs. (1) and (2) ought be by using the self-consistent mean-field Maier-Saupe theory of the nematic state. We shall not dwell into the details of the Maier-Saupe theory, which is described in the overwhelming majority of the classical books [22–25] and reviews [26] in the field, but rather describe its usage for our present purposes. We avoid the self-consistent calculation [22,23] of the distribution function $f(\Theta)$ and the order parameter $S(T) = -1/2 + 3/2 \langle \cos^2(\Theta) \rangle_T$ by using a simplified analytic form for $S(T)$ like [24]

$$S(T) \sim (1 - T/T_c)^{0.22}, \quad (3)$$

which reproduces fairly well the general shape of the self-consistent $S(T)$ obtained numerically from the Maier-Saupe theory and neglects the variation of the molar volume with temperature. Once $S(T)$ is known, the distribution function $f(\Theta)$ can be evaluated and the averages in Eqs. (1) and (2) obtained. This is shown in Fig. 1(b) (solid symbols) for both I_{\parallel} and I_{\perp} . We have chosen a range of reduced temperatures $t = T/T_c$ which agrees with the temperature range of the experiments we shall describe in the next subsections. The interpretation of the curves in Fig. 1(b) is quite simple: for the parallel excitation, the increase in temperature results in a broader spread of orientations around \vec{n} in view of the decrease in $S(T)$. The molecules are less excited by the incident laser, and also their emission along the vertical direction (parallel to \vec{n}) is less effective. Quite the opposite occurs for the perpendicular excitation, where the spread around \vec{n} helps in both the absorption and emission of the dyes. At $T = T_c$ the two curves combine, as expected from an isotropic distribution of orientations.

Indeed, this simple model of the dyes guided by the molecular order of the nematic LC does take into account the *orientational* aspects of the light absorption and emission processes, but falls short of considering the fact that the fluorescence emission efficiency generally decreases with temperature. The latter is a natural consequence of the increase in nonradiative recombination pathways for the excited molecules. The decrease in the fluorescence efficiency can be modeled by a prefactor of the form [27]

$$I_0(T) = I_0(1 - e^{-T^*/T}), \quad (4)$$

where $k_B T^* \equiv U$ represents the characteristic or average energy of the excitations participating in nonradiative recombination channels. Equation (4) will therefore be a prefactor for the orientational contributions in Eqs. (1) and (2). In Fig. 1(b) we show qualitatively the combined result of $S(T)$ and the nonradiative processes on the overall shape of the lumi-

nescence emitted by the dyes (open symbols) for both I_{\parallel} and I_{\perp} . In Sec. II B, we present an experimental attempt to verify the predictions of this simple model, and underscore those features that do not suit this description and go beyond its scope.

B. Sample preparation

The sample for our experiment was made from a mixture of the nematic liquid crystal E_7 (Merck) and the dye 3,3'-diethylthiadicarbocyanine iodide (DTDCI). E_7 is a nematogen mixture of 4-alkyl-4'-cyanobiphenyls and terphenyls [28] with a wide nematic range (~ -10 – 63 °C) and negligible residual absorption in the visible and near infrared. DTDCI is one of the classic cyanines that have been studied since the early days of molecular physics applied to dyes [29]. The sample was prepared with a dye concentration of 10^{-3} mg/ml accomplished by successive dilutions. The planar alignment of the cell was achieved by the Chatelain method [30] of rubbing the cell windows along a fixed direction. A $100\text{-}\mu\text{m}$ mica spacer is used between the two scraped windows to form the cell that allows transmission experiments to be performed. The alignment of the cell was tested by a birefringence measurement at room temperature ($T = 23$ °C) between crossed polarizers [31]. A white light source from a dichroic lamp with a very low power density on the sample ($< 1 \mu\text{W}/\text{mm}^2$) was collimated from a long distance with pinholes and transmitted through the LC cell. The sample is placed in between two crossed polarizers at 45° with respect to \vec{n} . The transmitted light is analyzed by a Jobin-Yvon T64000 triple spectrometer working in a subtractive mode and coupled to a photomultiplier. The data are shown in Fig. 2(a) for the visible range ~ 450 – 800 nm. The analysis of the curve follows that of Ref. [32]. If the birefringence Δn is dispersionless (i.e., it does not depend on the photon energy ω), then indexing the peaks by successive integers as a function of their energy position should bear a straight line. This is shown in the inset of Fig. 2(a) not to be the case, revealing that there is a weak but noticeable effect of dispersion in this energy range. Inasmuch as we are interested in a rapid characterization of the cell, we can assess a maximum value [32] for Δn of ~ 0.2 which is in excellent agreement with the technical data for this LC. It is important to note that the incident polarization of the laser that excites the dyes in the fluorescence experiment we shall describe later is always kept either perpendicular or parallel to \vec{n} . The idea is precisely to avoid the effect of the birefringence which would introduce an unnecessary complication for the analysis of how the dyes are being excited.

In Fig. 2(b) we show the absorption and fluorescence spectra of DTDCI in ethanol, measured with a white light source and a He-Ne laser excitation, respectively. The characteristic Stokes shift between the maxima of the fluorescence and absorption can be seen. The details of the spectra are explained elsewhere [29]. The selection of this particular dye was made because it can be resonantly excited by a He-Ne laser near the maximum of the absorption, thus facilitating experimentation.

C. Fluorescence decay, photobleaching, and diffusion

The first drawback one encounters when the doped LC cell is prepared, and the He-Ne laser is pumping the dyes

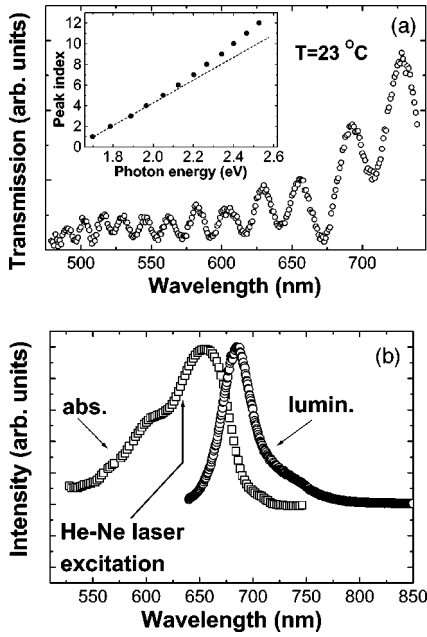


FIG. 2. (a) Transmission between crossed polarizers in the visible range for an E_7 sample doped with DTDCI. Note the presence of maxima and minima due to the birefringence. The sample thickness was $100 \mu\text{m}$. The inset shows the energy position of the peaks as a function of an integer index. The line shows that a linear fit for the first three points cannot match the rest of the data points, showing the presence of dispersion in Δn . This allows us to obtain a maximum value for Δn of 0.2. (b) Absorption and fluorescence spectra of DTDCI in ethanol. Note that the maximum of the fluorescence is at $\sim 695 \text{ nm}$, and that the dye can be resonantly excited almost at the maximum of the absorption by a He-Ne laser (shown with an arrow).

with a fixed polarization, is a drift of the fluorescence signal that persist for several seconds or minutes depending on the laser power density. This effect occurs at a fixed temperature, and its understanding is, therefore, a prerequisite for the observation of the temperature dependence of the fluorescence predicted in Fig. 1(b). We attribute this phenomenon to the presence of photobleaching, based on reasons we make clear in this subsection.

In Fig. 3 we show the decay of the fluorescence signal measured at the maximum of the emission $\sim 695 \text{ nm}$ [see Fig. 2(b)] with a He-Ne laser excitation of $1600 \mu\text{W}/\text{mm}^2$ for both, parallel and perpendicular excitations at $T = 23^\circ\text{C}$. The signal is at the beginning larger for I_{\parallel} as expected from Eqs. (1) and (2), and remains larger for subsequent times. Both fluorescence signals have a pronounced decay in 1800 sec at these relatively large power densities and, furthermore, we show in Fig. 3 the effect of interrupting the laser excitation for another 1800 sec and set it going afterward. We observe that there is a partial recovery of the fluorescence with respect to its value at $t=0$, but there is some sort of *memory effect* in the lighted up region. This is shown in Fig. 3 for I_{\perp} only, but the same phenomenon occurs for I_{\parallel} . Depending on the power density under consideration, one may have to wait up to 2–3 h for a total recovery of the fluorescence at room temperature.

In Figs. 4(a)–4(b), we show two additional and related aspects of this drift in the fluorescence. Figure 4(a) shows

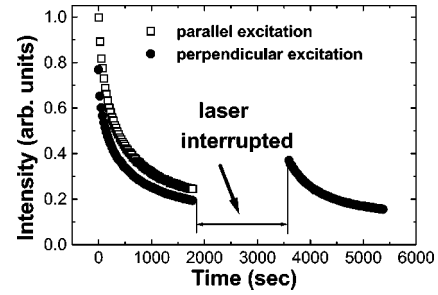


FIG. 3. Fluorescence decay for both excitations at a fixed temperature of $T = 23^\circ\text{C}$ and a power density of $1600 \mu\text{W}/\text{mm}^2$. Note that the two signals wane, but keeping $I_{\parallel} > I_{\perp}$. The power density used here is relatively high with respect to the ones we used for the temperature dependence of the fluorescence afterward. The laser runs for 1800 sec on the sample, and is then interrupted for another 1800 sec for I_{\perp} . If turned on again, there is only a partial reestablishment of the fluorescence with respect to its value at $t=0$. This time is related to the diffusion of photobleached molecules at the laser spot.

several fluorescence signals (normalized by their values at $t = 0$) for different power densities as a function of time at $T = 23^\circ\text{C}$. The data are taken for the perpendicular excitation condition. It is clearly shown that the decay time becomes smaller for larger power densities. On the other hand, Fig. 4(b) displays the decay times obtained from exponential fits to the data for both I_{\parallel} and I_{\perp} . Note that τ_{\perp} is systemati-

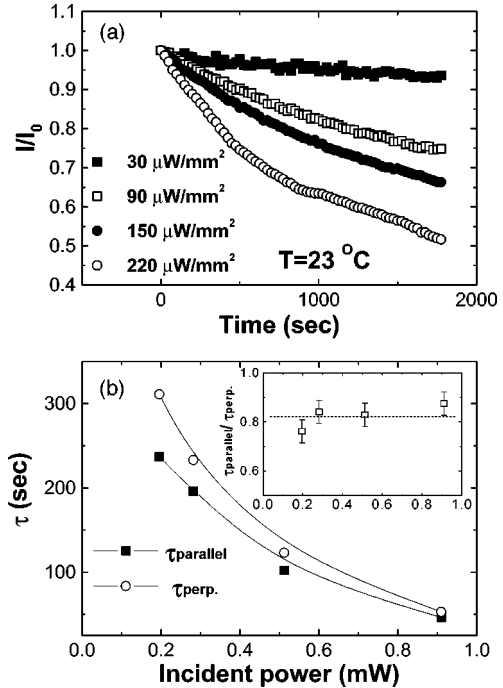


FIG. 4. (a) $I_{\perp}(t)/I_{\perp}(t=0)$ for different incident power densities at a fixed temperature of $T = 23^\circ\text{C}$. Note that the larger the power density the faster the drop of the signal relative to its value at $t = 0$. (b) Time constants τ_{\parallel} and τ_{\perp} as a function of incident power for I_{\parallel} and I_{\perp} , respectively. The area of the laser spot is the same for all the data points. Mind the fact that $\tau_{\parallel} < \tau_{\perp}$ but their ratio $\tau_{\parallel}/\tau_{\perp}$ is almost constant (inset). The dashed line in the inset is the prediction of $\langle \sin^4(\Theta) \rangle_T / \langle \cos^4(\Theta) \rangle_T$ from the Maier-Saupe theory at $T = 23^\circ\text{C}$. See the text for further details.

cally larger than τ_{\parallel} , suggesting that the decay is directly related to the amount of coupling between the laser and the dye molecules. Furthermore, their ratio $\tau_{\parallel}/\tau_{\perp}$ remains almost intensity independent, as shown in the inset of Fig. 4(b).

All these phenomena can be explained by the simultaneous presence of dye photobleaching and diffusion, as we shall explain here. A temperature rise or any other indirect thermal effect can be readily discarded as being responsible for the fluorescence decay. Typically, we use input powers of the order of ~ 0.1 mW distributed over an area of 2 mm in diameter and, due to the very low dye concentration, less than 1% of the total power will be absorbed. A very simple calculation for the steady-state temperature distribution using typical thermal conductivities for LC [26] shows that the temperature rise must be by all means negligible. In addition to the extremely low power being absorbed, a fluorescence recovery time in the illuminated area of more than half an hour (as shown in Fig. 3) cannot be explained by a thermal effect. In the photobleaching scenario, the laser illuminates an area of the LC cell and resonantly pumps the dyes. The photobleaching of the dyes occurs from the excited state of the molecules, and can be thought of as coming from a two concatenated steps process: (i) excitation of the dye, and (ii) photodissociation from the excited state. Thus the probability to photobleach a molecule P_{pb} is

$$P_{\text{pb}} \equiv \frac{1}{\tau_{\text{pb}}} = P_{\text{ex}} \times P_{\text{pd}}, \quad (5)$$

where P_{ex} and P_{pd} are the probabilities for excitation and photodissociation, respectively. Both P_{ex} and P_{pd} turn out to be proportional to the absorbed intensity I_{abs} . Moreover, since I_{abs} is different for the two excitation conditions \parallel and \perp to \vec{n} , we have two different relaxation times τ_{\parallel} and τ_{\perp} which, according to Eq. (5), should follow

$$\tau_{\parallel} \propto \frac{1}{I_0^2 \langle \cos^4(\Theta) \rangle_T}, \quad \tau_{\perp} \propto \frac{1}{I_0^2 \langle \sin^4(\Theta) \rangle_T}. \quad (6)$$

From Eq. (6) we observe that both τ_{\parallel} and τ_{\perp} are proportional to $1/I_0^2$. Moreover, $\tau_{\parallel}/\tau_{\perp} = \langle \sin^4(\Theta) \rangle_T / \langle \cos^4(\Theta) \rangle_T$, independent of I_0 and, in addition, $\tau_{\perp} > \tau_{\parallel}$ for $T < T_c$. All these features can be coarsely observed in the data of Fig. 4(b). Further, the dashed line in the inset of Fig. 4(b) shows the prediction for $\langle \sin^4(\Theta) \rangle_T / \langle \cos^4(\Theta) \rangle_T$ from the Maier-Saupe theory at $T = 23^\circ\text{C}$, with a T_c of 63°C corresponding to E_7 . This is, of course, under the assumption that the order parameter of the dye follows exactly that of the LC. Although the excellent quantitative agreement with the mean-field theory may be accidental, it is quite obvious that the fluorescence drift can be interpreted within this framework.

If the dye molecules were fixed in space, the illuminated area would undergo photobleaching until the number of molecules is exhausted and the fluorescence would approach zero. This situation is prevented by diffusion, and the final limiting value of the fluorescence at very long times will depend on the ability of the dyes to diffuse in and out of the illuminated region. This is, in fact, what produces the recovery of the signal after leaving off the laser for half an hour in

Fig. 3. In order to support this interpretation, we measure the *average* diffusion coefficient of DTDCI in E_7 in a separate experiment. Since this is not the main subject of this paper, we comment on the results and refer the reader to Ref. [33] for further details. We obtain an average diffusion coefficient of $\bar{D} = 1.0 \times 10^{-7} \text{ cm}^2 \text{ sec}^{-1}$ for DTDCI in E_7 at $T = 23^\circ\text{C}$, which is in excellent agreement with typical values for the self-diffusion coefficients in nematics [25]. For DTDCI in ethanol, on the other hand, the diffusion coefficient is $1.5 \times 10^{-5} \text{ cm}^2 \text{ sec}^{-1}$, two orders of magnitude larger. A simple estimation shows that this diffusion coefficient is in good agreement with the time the illuminated area of the sample needs to recover, taking into account that the molecules have to clear out photobleached molecules from a region of the order of 2 mm in diameter (a typical laser spot used in the experiments) and replace them by normal dye molecules. Conversely, the same experiment of Fig. 3 in a sample of DTDCI in ethanol recovers the same amount of fluorescence signal in 20 sec, which is two order of magnitude smaller than in E_7 , and in agreement with the ratio between their diffusion coefficients. In ethanol, of course, there is no polarization dependence for the absorption but, on the side of that, it is quite clear that diffusion and photobleaching are two intertwined aspects governing the fluorescence signal. Furthermore, the time constants observed experimentally, like those of Fig. 4(b), can be shown to be directly related to the fact that the dyes are being excited resonantly. For the same power densities, the relaxation times τ_{\parallel} and τ_{\perp} are two to three orders of magnitude larger when the exciting light is either the 514- or the 488-nm laser lines of an Ar^+ laser, respectively. The out-of-resonance excitation condition of these two lines [see Fig. 2(b)] results, accordingly, in a much lower fluorescence intensity when compared to the 633-nm line (He-Ne laser) for the same power density.

It is important to note that the decay time of the fluorescence observed experimentally will be given by an expression of the form of Eq. (6) only for sufficiently high input laser powers so that the photobleaching process dominates over the characteristic recovery time for diffusion τ_d . This turns out to be the case for the experimental conditions and temperature used here. Conversely, if the laser power is too small so that $\tau_d \sim \tau_{\parallel, \perp}$, the observed decay should follow an effective time constant of the form $1/\tau_{\text{eff}} = 1/\tau_{\parallel, \perp} + 1/\tau_d$ [33].

To finish this subsection we would like to remark that the observation of a coexistence between photobleaching and diffusion is, actually, not new, but rather comprises one of the well known techniques used in several branches of biology, and is known as *fluorescence photobleaching recovery spectroscopy* (FPRS) [34]. The technique is mainly used to study the diffusion of fluorescently tagged dextrans or proteins through different types of tissues [34]. The new feature added in LC case is, perhaps, the fact that the absorption is anisotropic due to the intrinsic order of the nematic state in an oriented sample. Furthermore, it is also possible to image the photobleaching and diffusion processes by working directly in a *double subtractive* mode with the monochromator, and forming an image of the output of the second stage directly onto a charge coupled device (CCD) array. The technique depends on the illumination of the sample by two HeNe laser beams: one with low intensity and expanded

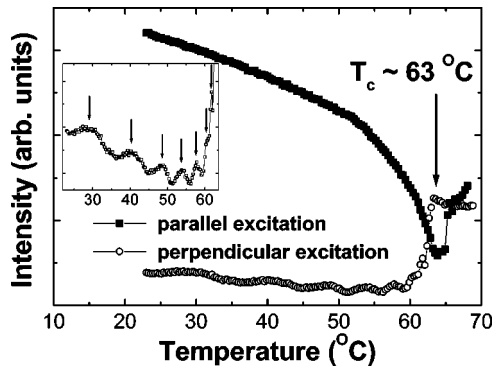


FIG. 5. Polarized fluorescence as a function of temperature for an incident power density of $150 \mu\text{W}/\text{mm}^2$. This result should correspond to the predicted curves in Fig. 1(b) (open symbols). Note that the main qualitative differences with the prediction in Fig. 1(b) are (i) the behavior near T_c , and (ii) the presence of oscillations in I_{\perp} . The inset is an enlargement of the data for I_{\perp} showing that the distance between peaks shrinks when T_c is approached from below.

(which serves as a probe), and one with high intensity and focused on a reduced area within the first beam. The contrast between the photobleaching effect of the former with respect to the latter can be directly seen in the image which is filtered at the emission of the dyes by the double subtractive monochromator. These experiments have been performed, and are further inquired into elsewhere [33].

In Sec. IID, we shall be dealing with the temperature dependence of the fluorescence signals. However, we shall never be using a power density as high as that used in Fig. 3. In any case, *we understand hereafter that the fluorescence signals are those obtained once the initial decay is completed, and an equilibrium condition is established between photobleaching and diffusion.*

D. Temperature dependence of the polarized fluorescence

Once the photobleaching problem is accepted, we are now in a position to sweep the temperature and observe the effect of $S(T)$ on the fluorescence signals of the dyes for both I_{\parallel} and I_{\perp} . This is shown in Fig. 5 at a power density of $150 \mu\text{W}/\text{mm}^2$. The following features should be observed in the data: (i) the general qualitative agreement with the prediction of Fig. 1(b) (open symbols) is good. The parallel excitation shows a continuous decay up to the transition to the nematic state, while I_{\perp} displays a mild decrease followed by an increment near T_c . (ii) The intensities of I_{\parallel} and I_{\perp} for $T > T_c$ are almost equal in the isotropic state, as expected, but the data have a more complicated behavior at and near T_c which is not predicted by the model in Sec. IIA. (iii) I_{\perp} displays clear oscillations in the experimental data as function of temperature. The inset of Fig. 5 shows the details of these oscillations and the fact that the distance between successive peaks contracts when T_c is approached from below.

The fact that the data for I_{\perp} and I_{\parallel} in Fig. 5 behave differently from the prediction in Fig. 1(b) near T_c is not at all surprising if we take into account that the averages in Eqs. (1) and (2) have been obtained from the Maier-Saupe theory. Most predicted qualitative features of a mean-field theory are expected to fail near T_c , where fluctuations dominate. This

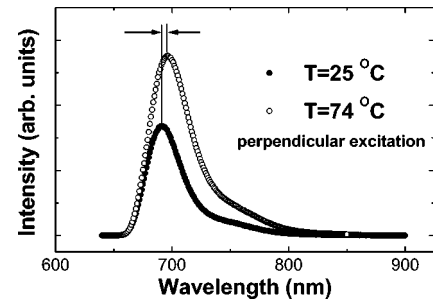


FIG. 6. Fluorescence signal for I_{\perp} as a function of wavelength for two temperatures in the nematic (open circles) and isotropic (full circles) states. Note that there is a shift of the maximum of ~ 4 nm between these two temperatures and that $I_{\perp}(T=25^{\circ}\text{C}) < I_{\perp}(T=74^{\circ}\text{C})$, showing the explicit contribution of the nematic order which diminishes both the excitation and the emission at $T=25^{\circ}\text{C}$ with respect to $T=74^{\circ}\text{C}$.

is one of the most salient and well known shortcomings of the mean-field approach to phase transitions. The detailed light dispersion near T_c , i.e., around the clearing point [23], undoubtedly requires a more rigorous treatment of the transition.

Conversely, the existence of oscillations in the signal for I_{\perp} is very interesting and cannot be ascribed to a serious weakness of the mean-field theory but rather to a missing ingredient in the description. In Sec. III, we shall present a model that accounts for the experimental observations which is based on the existence of a resonant optical torque twisting the dye molecules with respect to the main dielectric axes of the LC. For the time being, however, we shall present a few more experimental facts to characterize the behavior of these oscillations.

Since we are taking the maximum of the fluorescence signal [see Fig. 2(b)] as representative for the emission intensity of the dyes, we may worry about possible temperature shifts of the peak influencing the signal in Fig. 5. It is well known that the maximum of a homogeneous fluorescence peak should both move toward larger wavelengths, and its intensity should fall when T is increased. In Fig. 6 we show two fluorescence peaks in the nematic ($T=25^{\circ}\text{C}$) and isotropic ($T=74^{\circ}\text{C}$) phases as a function of wavelength. Both curves are obtained for the horizontal excitation condition, with a higher resolution (0.5 nm) than the one we normally use to measure the intensity at the maximum (~ 8 nm). Two interesting features can be seen in the data: (i) the maximum of the peak shifts by ~ 4 nm from 25 to 74°C , and (ii) the intensity of the peak is larger for $T=74^{\circ}\text{C}$ in this particular excitation. The fact that the maximum is displaced by only 4 nm in the whole temperature range of our experiments, and that we measure the intensity of the fluorescence at 695 nm with a resolution of 8 nm, tells us that we can ignore the temperature shift of the peak as being responsible for any of the features in Fig. 5 and the forthcoming figures. Changes in the fluorescence signal at a fixed wavelength of 695 nm come essentially from variations in the peak intensity at the maximum. Moreover, for a fluorescence to reduce its intensity at higher temperatures on account of the increase of nonradiative recombination processes is not surprising, but Fig. 6 shows exactly the opposite: $I_{\perp}(T=74^{\circ}\text{C}) > I_{\perp}(T=25^{\circ}\text{C})$. The latter is the result of

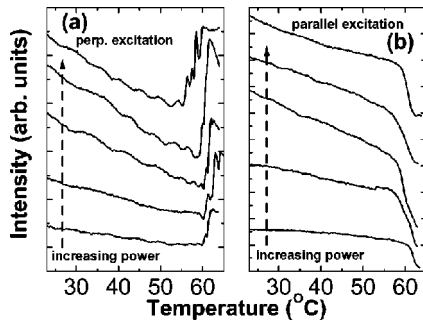


FIG. 7. Fluorescence emission for I_{\perp} (a) and I_{\parallel} (b) at 695 nm, as a function of temperature for different input power densities. For both graphs we used (from bottom to top) 30, 60, 90, 120, and 150 $\mu\text{W}/\text{mm}^2$ with the 633-nm He-Ne laser line as excitation. Note that I_{\parallel} shows no oscillations while I_{\perp} displays oscillations with increasing amplitude for higher power densities. Note also that the amplitudes of the oscillations for a fixed power density are somewhat larger near T_c . See the text for further details.

the order imposed by the LC on the dyes and a direct view into the consequences of Eq. (2), which gives $\langle \sin^4(\Theta) \rangle_{T=74^\circ\text{C}} > \langle \sin^4(\Theta) \rangle_{T=25^\circ\text{C}}$.

Having said this, we continue in Figs. 7 and 8 with a further characterization of the oscillations in I_{\perp} as a function of temperature. It has been established that oscillations appear only in I_{\perp} and not in I_{\parallel} , and that their amplitude swells with increasing input power density. This is shown in Fig. 7, where a series of temperature scans are shown for I_{\perp} and I_{\parallel} for different input power densities at 633 nm. As can be readily seen, oscillations appear in I_{\perp} with increasing amplitude for higher power densities, but they never come in view for I_{\parallel} . Further, we can see in Fig. 7(a) that the relative amplitude of the oscillations seems to be larger for temperatures close to T_c than far from the transition. In addition in Fig. 8 we show the result of changing the input laser wavelength on the fluorescence signal for I_{\perp} for a fixed power density of 150 $\mu\text{W}/\text{mm}^2$. Note that, as explained in Sec. II C, the 488-

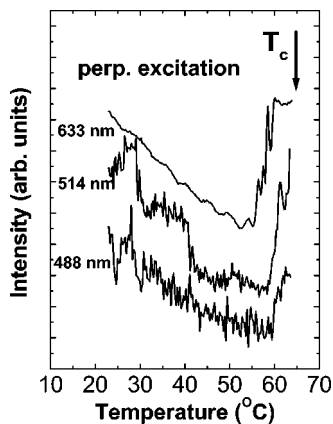


FIG. 8. I_{\perp} as a function of T for three different exciting laser lines—633, 514, and 488 nm—with the same power densities (150 $\mu\text{W}/\text{mm}^2$). The signal is smaller for 514 and 488 nm due to the lower absorption of the dye [see Fig. 2(b)]. In addition, there is no sign of oscillations in the data for 488 nm and perhaps one visible peak near T_c for 514 nm. The data for 633 nm show very clear evidence of oscillations. The data are consistent (but not conclusive), with a resonant torque put forth by the laser onto the dyes.

and 514-nm lines of the Ar^+ laser excite the dye out of resonance. As a consequence, the signal to noise ratio worsens, as can be seen in Fig. 8. Notice that no oscillations can be seen in the fluorescence data for 488 nm, while there is one visible peak near T_c for 514 nm. With the 633-nm excitation line, the oscillations are clearly visible. One may argue that the oscillations in the signal exist for the 488- and 514-nm lines, but the signal to noise ratio does not allow their observation. However, as we shall explain in Sec. III, we believe that these data indicate a resonance effect in the interaction producing the oscillations. In Sec. III, we deal with a simple model that combines the existence of a resonant optical torque and the LC elastic energy to account for these observations.

III. DISCUSSION

In order to develop an explanation that accounts for the experimental findings and the missing ingredients of the model in Sec. II A, we need to stress a few very basic facts on top of which we shall develop the description. It is very important to realize the necessary conditions required to observe oscillations in the fluorescence as in Fig. 5. If the dye molecules remained aligned exactly in the direction of \vec{n} , i.e., following strictly the order parameter of the nematic $S(T)$, the birefringence of the LC would never be seen by the fluorescence of the dyes irrespective of the orientation of the LC cell with respect to the polarizers. It is a straightforward exercise of classical optics [31] in the plane wave approximation to show that in order to perceive the birefringence of a sample in a transmission experiment between crossed polarizers, the *light source* must be polarized at some angle with respect to the principal dielectric axes. Additionally, the output polarizer preceding the detector (see Fig. 1) must not be aligned with the principal dielectric axes to observe the birefringence. The experiment performed in Sec. II B to characterize the birefringence of the LC cell with two crossed polarizers at 45° with respect to \vec{n} is nothing but a special case of these two conditions. The main difference with the experiment of Sec. II B is that the observed light does not come from an external white light source, but that it is rather generated inside the sample through the fluorescence of the dyes.

The model that describes all the basic features observed in the experiment is as follows: there is a resonant optical torque that competes with the internal elastic energy forced upon the dyes by the LC. The torque has no effect when the polarization of the laser \vec{E}_l is \parallel to \vec{n} . If $\vec{E}_l \perp \vec{n}$, however, the dyes are left in an unstable situation trying to cope with both the elastic energy interaction with the LC and the potential energy of the interaction with the laser. Although the torque itself is zero for \vec{E}_l strictly \perp to \vec{n} , the potential energy of the interaction with the laser is in a local maximum and, therefore, in an unstable condition. The reader may appreciate that this is, in fact, a simple generalization of one of the possible configurations of the Fréedericksz transition for static (dc) fields, albeit as a rule the extension to the optical frequencies has to be taken with care and justified by experimental evidence. The main problem is that LC's do not always behave in the same manner when the dc behavior is compared to the

bearing in the optical range, as demonstrated in the well-known examples of adiabatic propagation of light [35] or in optical Fréedericksz transitions that have no analog to dc fields [36]. If z is the propagation direction of the light, and Θ the departure angle of the dyes from \vec{n} in the direction perpendicular to z and parallel to the cell windows, we obtain the equilibrium condition as [23]

$$\frac{d}{dz} \left[k' \left(\frac{d\Theta}{dz} \right)^2 + \alpha(\omega) I \sin^2(\Theta) \right], \quad (7)$$

exactly as in the continuum theory of the Fréedericksz effect [23]. In Eq. (7), k' is the elastic constant between the dyes and the LC molecules, $I \propto E_l^2$ the intensity of the laser, and $\alpha(\omega)$ a function with a resonance at $\omega = \omega_0$, where ω_0 represents the photon energy where the dyes absorb. The fact that Eq. (7) governs the stability of the dyes within the LC deserves specific attention. There are two types of elastic interaction in the doped LC. The LC molecules interact among themselves, and this produces the standard Frank elastic constants [23] (k). On the other hand, there is an interaction between the dyes and the LC molecules which defines an *effective* elastic constant k' for the deformation of the former with respect to the latter. The origin of k and k' is at a molecular level. In a sense, the problem of twisting the dyes with respect to the LC internal order is similar to two masses connected by two springs, one between them and the other between one of the masses and a fixed reference wall. The first spring represents the elastic interaction between the dyes and the LC (k'), while the second serves as a model for the elastic interactions between the LC and the boundary conditions (k). By pulling from the first mass, representing the dyes, several situations are possible depending on the actual values of k and k' . If $k > k'$ the dyes can be twisted with respect to \vec{n} , while the LC may still obey the boundary conditions imposed by the cell. If $k < k'$, the LC will follow the twist of the dyes, and this type of *indirect torque* is responsible for many of the phenomena reviewed in Sec. I. In addition, if $k \sim k'$, both the dyes and the LC can be twisted with respect to cell but not necessarily by the same amount. We believe that the situation for our sample and experimental conditions can best be modeled by either $k' < k$ or $k' \sim k$. In this way, Eq. (7) represents, the equilibrium of the dyes in their interaction with the LC and the optical field.

The main difference between Eq. (7) and the dc Fréedericksz effect is perhaps the fact that $\alpha(\omega)$ is a resonant function at $\omega = \omega_0$, coming from the interaction of \vec{E}_l and the dynamic polarization induced by \vec{E}_l on the dye molecules. This has drastic consequences for the threshold condition of the twist which is proportional to $\sqrt{k'/\alpha(\omega)}$ and can, therefore, be very small. Indeed, we believe that this, together with $k' < k$, are the conditions that actually allow the twist of the dyes with respect to the LC to be observed. The laser couples strongly to the dyes but, at the same time, it is too weak to produce by itself a direct modification of the LC, as seen in the well known examples of optical reorientations [24].

A dye molecule emitting fluorescence at a distant z from the end face of the cell and with a twist angle Θ with respect

to \vec{n} will produce a state of polarization at the output that contains information on the birefringence $\Delta n(T)$ of the LC at a given temperature T . The second condition needed to observe the birefringence, i.e., the direction between \vec{n} and the output polarizer, can be fulfilled by either a small misalignment of the output polarizer if $k' < k$, or by a small twist of the director \vec{n} if $k' \sim k$. We cannot distinguish between these two situations experimentally. In any event, provided that both conditions are accomplished, the signal at the detector contributed by the molecule will be of the form [31]

$$I \sim \left[1 + C(\Theta, \omega, I) \cos \left(\frac{2\pi \Delta n(T) z}{\lambda} \right) \right], \quad (8)$$

where λ is the wavelength of the light in vacuum and $C(\Theta, \omega, I) \propto \alpha(\omega) I$. If Θ were 45° , then $C(45^\circ) = 1$, reducing Eq. (8) to $I \sim \cos^2(\pi \Delta n(T) z / \lambda)$, which is the well-known formula [31] for a birefringent medium between crossed polarizers. Likewise, the total contribution to the signal comes from all the fluorescence emissions along the cell of thickness d . The emissions are incoherent among each other because the fluorescence decay implies a relaxation process through internal excitations (vibrations, etc.), and these lose phase information from the exciting laser. The total contribution to the signal must be calculated, accordingly, as a sum of partial intensities for different z 's given by Eq. (8), and not their electric fields, as would be the case if coherence subsisted.

By taking into account the effect of the torque as a small perturbation to the contributions given by Eqs. (2) and (4), we arrive at a total intensity of the form

$$I_{\perp} \sim \left[1 + \frac{A}{\Delta n(T)} \sin \left(\frac{2\pi \Delta n(T) d}{\lambda} \right) \right] (1 - e^{-T^*/T}) \langle \sin^4(\Theta) \rangle_T, \quad (9)$$

where the first expression between brackets is the integrated effect of Eq. (8) (properly normalized by the first term), the second and third expressions come from Eqs. (4) and (2), respectively, and $A \equiv C(\Theta, \omega, I) \lambda / 2\pi$ is a constant for a given laser intensity and frequency. Equation (9) has two adjustable parameters: A , which fixes the *amplitude* of the oscillations, and T^* , which corrects the downward shift of the signal due to nonradiative recombinations. For $\Delta n(T)$ we take the simplest possible model given by [23]

$$\Delta n(T) \equiv \Delta n(0) \times S(T), \quad (10)$$

with $\Delta n(0) = 0.2$, suggested by the data in Fig. 2(a), and $S(T)$ given by Eq. (3). In Fig. 9 we plot the prediction of Eq. (9) together with the experiment. We took a value of A that approximately reproduces the amplitude of the oscillations as well as an appropriate value of T^* . Notice also that the number of peaks in the whole temperature range, related to the value of $\Delta n(0)$, is fairly well reproduced, since ten peaks are clearly seen in the model calculation and nine are observed experimentally.

In addition to the qualitative agreement in Fig. 9 there are a few more aspects that can be interpreted by Eq. (9): (i) the data in Fig. 8 can be explained by the resonant enhancement of $A \propto \alpha(\omega)$, which increases the amplitude of the oscilla-

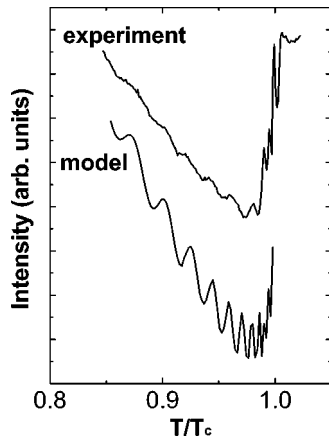


FIG. 9. Experiment (with the 633-nm excitation) and model [from Eq. (9)] for I_{\perp} . The model takes into account the average orientation from the mean-field theory [Eq. (2)], the nonradiative recombinations from Eq. (4), and the existence of a twist given by the integrated effect of Eq. (8).

tions; (ii) the fact that $\alpha(\omega)$ can be large for $\omega \sim \omega_0$ may explain why the twist of the dyes has a very low threshold, and can be observed at very low power densities, as seen in Fig. 7(a); and (iii) the amplitude of the oscillations depends on temperature like $(1/\Delta n(T))\sin(2\pi\Delta n(T)d/\lambda)$, which gives larger amplitudes for $T \rightarrow T_c$. This may explain why the amplitudes seem to be relatively larger close to T_c , as can be seen in Figs. 7–9.

We judge the qualitative agreement between the model and the experiment in Fig. 9 as excellent, and we regard it as clear proof of the existence of a laser induced twist of the dyes with respect to the LC host. This selective twist has not been heretofore reported in the literature, to the very best of our knowledge.

To finish this discussion, we would like to comment on two possible effects that were not included by virtue of the Ockham's razor principle, namely, the possible effects of the

temperature dependence of the diffusion and elastic constants. The equilibrium value of the photobleached signal in Sec. II C, as well as the final stable twist angle in Eq. (7), may change slightly if \bar{D} and k' depend on temperature. These variations are probably needed to explain the fine details of the data in Fig. 5 close to the clearing point. Still, it is quite clear from Fig. 9 that the gross features of the data, except very close to T_c , can be easily explained without these ingredients.

IV. CONCLUSIONS

We have studied the resonant interaction of dyes dissolved in a prototype LC. For the particular dye we used (DTDCI), we found evidence in the early stages of the laser illumination of polarized photobleaching coexisting with dye diffusion through the nematic host. In addition, by way of the temperature dependence of the polarized fluorescence, we found evidence of the existence of a resonant torque acting on the dyes and twisting their orientation with respect to the principal axes of the LC director. The temperature dependence of the birefringence can be seen in this latter case by the dye fluorescence as oscillations in the detected intensity. We hope that our results will help to augment and clarify some of the basic aspects of light interactions with dye doped LC.

ACKNOWLEDGMENTS

Special thanks are due to F. Tutzauer, R. Gludovats, C. Eggenchwiler, R. Soto, and B. Eckardt for the construction and design of different parts of our experimental setup. It is also a pleasure to thank A. Fainstein for stimulating discussions, several hints, and ideas for the modeling and interpretation of the experimental data, and for a critical reading of the manuscript. M.N. and D.S. acknowledge financial support from the Comisión Nacional de Energía Atómica of Argentina at the Instituto Balseiro. P.E. thanks the Fundación Antorchas for financial support through a reentry grant.

-
- [1] G. H. Heilmeyer, J. A. Castellano, and L. A. Zaroni, in *Proceedings of the International Liquid Crystal Conference* (Gordon, New York, 1968), Vol. 2-2, p. 763.
 - [2] M. Morita, S. Imamura, and K. Yatabe, *Jpn. J. Appl. Phys.* **14**, 315 (1975).
 - [3] G. H. Heilmeyer and L. A. Zaroni, *Appl. Phys. Lett.* **13**, 91 (1968).
 - [4] H. J. Coles, H. F. Gleeson, and J. S. Kang, *Liq. Cryst.* **5**, 1243 (1989).
 - [5] I. Jánossy and L. Csillag, *Phys. Rev. A* **44**, 8410 (1991); I. Jánossy, *Phys. Rev. E* **49**, 2957 (1994).
 - [6] I. Jánossy in *Proceedings of the NATO Advanced Resonance Workshop*, edited by F. Kajzar, V. M. Agranovich, and C. Y. C. Lee (Kluwer, Dordrecht, 1996), p. 477.
 - [7] I. C. Khoo, H. Li, and Yu Liang, *IEEE J. Quantum Electron.* **QE-29**, 1444 (1993); see also H. Li, Yu Liang, and I. C. Khoo, *Mol. Cryst. Liq. Cryst.* **251**, 85 (1994).
 - [8] D. Bauman and E. Wolarz, *Z. Naturforsch., A: Phys. Sci.* **51A**, 1192 (1996).
 - [9] J. W. Wu, *Nonlinear Opt.* **15**, 55 (1996).
 - [10] L. M. Blinov, M. V. Kozlovsky, M. Ozaki, and K. Yoshino, *Mol. Mater.* **6**, 235 (1996).
 - [11] I. Jánossy and T. Kosa, *Opt. Lett.* **17**, 1183 (1992).
 - [12] R. Münster, M. Jarasch, X. Zhuang, and Y. R. Shen, *Phys. Rev. Lett.* **78**, 42 (1997).
 - [13] T. Furukawa, T. Yamada, K. Ishikawa, H. Takezoe, and A. Fukuda, *Appl. Phys. B: Lasers Opt.* **60**, 485 (1995).
 - [14] J. Kato, I. Yamaguchi, and H. Tanaka, *Opt. Lett.* **21**, 767 (1996).
 - [15] T. Inoue and Y. Tomita, *J. Opt. Soc. Am.* **13**, 1916 (1996).
 - [16] H. Ono and N. Kawatsuki, *Jpn. J. Appl. Phys., Part 2* **36**, L353 (1997); *Appl. Phys. Lett.* **70**, 2544 (1997).
 - [17] A. G. Chen and D. J. Brady, *Appl. Phys. Lett.* **62**, 2920 (1993).
 - [18] F. Simoni, O. Francescangeli, Y. Reznikov, and S. Slusarenko, *Opt. Lett.* **22**, 549 (1997).
 - [19] S. Bartkiewicz and A. Miniewicz, *Adv. Mater. Opt. Electron.* **6**, 219 (1996).

- [20] T. Kosa and P. Palfy-Muhoray, *Pure Appl. Chem.* **5**, 595 (1996).
- [21] W. M. Gibbons, P. J. Shannon, S. T. Sun, and B. Swetlin, *Nature (London)* **351**, 49 (1991).
- [22] P. G. deGennes, *The Physics of Liquid Crystals* (Clarendon Press, Oxford, 1974).
- [23] S. Chandrasekhar, *Liquid Crystals* (Cambridge University Press, New Rochelle, NY, 1980).
- [24] I. C. Khoo, *Liquid Crystals, Physical Properties and Nonlinear Optical Phenomena* (Wiley Interscience, New York, 1995).
- [25] L. M. Blinov, *Electro-Optical and Magneto-Optical Properties of Liquid Crystals* (Wiley Interscience, Chichester, 1983).
- [26] M. J. Stephen and J. P. Straley, *Rev. Mod. Phys.* **46**, 617 (1974).
- [27] This is the same type of temperature dependence expected in the luminescence of direct band gap semiconductors through the interaction with the optical phonon of $\vec{k}=0$; see, for example, P. Yu and M. Cardona, *Fundamentals of Semiconductors, Physics and Materials Properties* (Springer, Heidelberg, 1996), and references therein.
- [28] Purchased from Merck, Poole, England.
- [29] L. G. S. Brooker, *Rev. Mod. Phys.* **14**, 275 (1942).
- [30] P. Chatelain, *Bull. Soc. Fr. Mineral. Cristallogr.* **66**, 105 (1943); J. L. Lanning, *Appl. Phys. Lett.* **21**, 15 (1972); D. Berreman, *Phys. Rev. Lett.* **28**, 1683 (1972).
- [31] A. Yariv, *Optical Electronics* (Saunders HBJ, New York, 1991), p. 24; *Quantum Electronics* (Wiley, New York, 1989).
- [32] A. Fainstein, P. Etchegoin, P. V. Santos, M. Cardona, K. Töttemeyer, and K. Eberl, *Phys. Rev. B* **50**, 11 850 (1994).
- [33] P. Etchegoin, following paper, *Phys. Rev. E* **59**, 1860 (1999).
- [34] X. H. Xu and E. S. Yeung, *Science* **275**, 1106 (1997); N. B. Cole, C. L. Smith, N. Sciaky, M. Terasaki, M. Edidin, and J. Lippincott-Schwartz, *ibid.* **273**, 797 (1996), and references therein. See also J. Manni, *Biophotonics* **3**(1), 44 (1996) for current trends involving FPRS with two-photon scanning microscopy.
- [35] L. Csillag, I. Jánossy, V. F. Kitaeva, N. Kroó, N. N. Sobolev, and A. S. Zolotko, *Mol. Cryst. Liq. Cryst.* **78**, 173 (1981); see also I. Jánossy, in *Optical Effects in Liquid Crystals*, edited by I. Jánossy (Kluwer, London, 1991).
- [36] E. Santamato, G. Abbate, P. Maddalena, and Y. R. Shen, *Phys. Rev. A* **36**, 2389 (1987).